COHERENT TURBULENT STRUCTURES IN A QUASI-STEADY SPILLING BREAKER

S. K. Misra[1], J. T. Kirby[1], M. Brocchini[2], F. Veron[3], M. Thomas[4] & C. Kambhamettu[4]

Abstract: In this paper, we analyze planar Particle Image Velocimetry (PIV) data of a laboratory hydraulic jump to investigate the large-scale coherence in the turbulent breaker shear layer. Two-point spatial correlations are used at various spatial locations to qualitatively assess the shape of the coherent structures in the different flow regimes. The structures are found to be stretched parallel to the mean surface in the form of ellipses, oriented along the mean strain rate near the foot of the breaker, and further downstream, become increasingly compact and oriented normal to the surface. This indicates the reduced efficiency of the coherent structures away from the foot in extracting energy from the mean flow. In addition, quantitative estimates of length scales are obtained from the correlation coefficients. The average length scales are found to be in the range of previously reported estimates for laboratory generated plunging and spilling breaking waves.

INTRODUCTION

An understanding of the turbulent flow in breaking waves is essential towards modeling the dynamics of the surf-zone. The post-breaking phase, because of the complexity of the resulting turbulent flow (being two-phase and highly intermittent), remains difficult to investigate, both theoretically (Svendsen and Madsen, 1984) and experimentally (Duncan, 2001; Govender *et al.*, 2002). Owing to the limited knowledge of the detailed dynamics, spilling breakers in the surf-zone are typically modeled as a stagnant eddy or roller riding on the front face of a wave (Madsen and Svendsen, 1983; Cointe and Tulin, 1994). An alternative qualitative description of the breaker shear layer and its turbulence structure suggests the generation of an intense "breaker mixing layer", which starts from the foot of the breaker (defined according to Brocchini and Peregrine (2001) as the ensemble averaged location of the toe) followed by a wake further downstream (Peregrine and Svendsen, 1978; Battjes and Sakai, 1981). In these "bulk" models, the turbulent structure of the flow, especially the details in the breaker shear layer and in the highly intermittent region near the surface, is either grossly simplified or completely disregarded.

[1]Center for Applied Coastal Research, University of Delaware, Newark, DE 19711, USA, shubhra@coastal.udel.edu

[2]D. I. A. M., Universita' di Genova, Via Montallegro 1, 16145 Genova, Italy

[3]Graduate College of Marine Studies, University of Delaware

[4]VIMS Lab, Dept. of Computer and Information Sciences, University of Delaware

There are, however, dominant and persisting energy containing scales in turbulent flows that exhibit evident structure, and these are called coherent structures. Laboratory experiments have clearly confirmed the existence of such classes of eddies in breaking waves (Nadaoka, 1986; Chang and Liu, 1998; Stansby and Feng, 2005). Non-intrusive whole-field measurement techniques such as PIV have aided the visualization and characterization of such organized motion in turbulent flows. Further, Melville *et al.* (2002) have shown that coherent structures in a deep water breaking wave can be studied using a mosaic of PIV images. With a light sheet in the streamwise-spanwise plane, PIV laboratory experiments conducted by Cox and Anderson (2001) on the breaking of regular plunging breakers revealed the nominal diameter (l) of (instantaneous) eddies associated with wave breaking to be around 0.05 m. The breaking wave-height (H_b) was 0.12 m which gives $\frac{l}{H_b}$ = 0.42. They noted that they could not detect larger eddies because of the restriction imposed by their target area, which was 10 cm $\times$ 10 cm. For many of their tests, they also found complex three-dimensional patterns with no well-defined eddies. Longo (2003), using orthogonal wavelets as a decomposition technique, found that more than 70 % of the total turbulent kinetic energy for spilling breakers were carried by micro (with a length scale in the range 2 mm $< l <$ 10 cm) and mid-size (10 cm $< l <$ 4.0 m) vortices, predominantly below the wave crest, and that most of the energy was transferred from the macro- and mid-size vortices to the micro-vortices after the passage of the breaker. The breaking wave-height was 10 cm, giving a maximum and minimum $\frac{l}{H_b} = 1$ for the micro- and mid-size vortices respectively. Stansby and Feng (2005), with laser Doppler anemometry experiments with laboratory generated bores, found multiple coherent vortices which were elongated along the surface.

Motivated by the analogy between quasi-steady surf-zone breakers and bores, recent analysis of a planar (streamwise-cross-stream) PIV study of a turbulent hydraulic jump has shown that the breaker shear layer can be characterized as a mixing layer (Misra *et al.*, 2005a). In this paper, we focus our attention on characterizing the large-scale coherent turbulent motions in the mixing layer. The experimental set-up and flow parameters are described in section 2. The two-point spatial correlation technique used to analyze the structure of the turbulence is described in 3. The results are presented in section 4 followed by conclusions.

EXPERIMENTAL SET-UP

The experiment was performed in a recirculating Armfield S6 tilting flume that is 4.8 m long and 30 cm wide, with glass side walls (9 mm thick) and an opaque bottom. The jump was set up downstream of a weir. The flow rate and the height of the weir are used to control the upstream flow velocity and water depth, thereby determining the upstream Froude number ($Fr = 1.2$). After passing the weir, the supercritical flow transitions to a subcritical flow by dissipating energy through the formation of an air-entraining hydraulic jump. The toe of the jump, defined here as the point of maximum surface curvature, was approximately 20 cm downstream of the weir. The flume was kept horizontal throughout the experiments.

The PIV set-up consisted of a 120 mj/pulse Nd-Yag New Wave solo laser source with a pulse duration of 3 to 5 nano seconds. This was mounted onto a custom-built submersible waterproof periscope which was lowered into the water. The optics were arranged in such a way that the laser beam emerged as a planar light sheet parallel to the flume wall. The water was seeded with 14 μm diameter silver coated hollow glass spheres with a specific

gravity of 1.8, obtained from Potters industries. A Kodak Megaplus 1.0 camera with a 1016 (vertical) $\times$ 1008 (horizontal) pixel CCD array, with its image plane parallel to the flume wall, was used to visualize the flow. A Dantec acquisition system was used to acquire the images and store them onto a hard drive. The laser pulses were synchronized with the 30 Hz camera frame rate, which ultimately led to a 15 Hz sampling rate for the instantaneous velocity fields. The time interval between two pulses in each image pair was 300 μ seconds. The target area of 11.17 cm (horizontal) $\times$ 11.09 cm (vertical) was focussed on the breaker shear layer. The instantaneous surface was estimated using image processing techniques and active contours (Misra *et al.*, 2005b). Each experimental run consisted of an ensemble of 1020 image pairs, equivalent to 1020 instantaneous velocity maps. The ensemble size was large enough to obtain satisfactory convergence of the turbulence statistics and the velocity vectors accurately satisfied global and local mass conservation in the whole domain. More details can be found in Misra *et al.* (2005a).

DOUBLE SPATIAL CORRELATIONS

The correlation operator is frequently used in the statistical approach of turbulent flows to investigate temporal or spatial coherence. A high degree of correlation indicates a deterministic link between otherwise random variables (such as the turbulent velocity fluctuations). The two-point spatial correlation, also known as the double spatial correlation, was first used for planar PIV data of wall turbulence by Stanislas *et al.* (1999) and has since been used to look at large-scale coherence in turbulent boundary layers for stereoscopic PIV data as well (Ganapathisubramani *et al.*, 2005). For two variables A and B, the spatial double correlation operator is defined as

$$R_{AB}(x, y, \delta x, \delta y) \equiv \frac{< A(x,y)\ B(x+\delta x, y+\delta y) >}{\sqrt{< A(x,y)^2 >}\ \sqrt{< B(x+\delta x, y+\delta y)^2 >}} \tag{1}$$

where x and y are respectively, in our case, the horizontal and vertical coordinates. $< \cdot >$ denotes an ensemble averaging over multiple realizations. δx and δy denote the horizontal and vertical distances between the "moving" point (B) and the "fixed" point (A). In the present case, A and B are the instantaneous velocity fluctuations (u or v, the horizontal and vertical components) obtained by removing the ensemble-averaged velocity from each instantaneous realization of the velocity field. Note that since the correlation is done at the same instant in the whole space, the hypothesis of frozen turbulence is removed, and there is, thus, no restriction on the evolution of the coherent structures (Stanislas *et al.*, 1999). For quasi-steady flow fields, R_{AB} is a function only of locations of A and B, and of the direction. So, for given locations and a given direction, R_{AB} has a fixed value. The form of the two-point correlation is, therefore, largely determined by the inhomogeneity of the flow field evident in the Reynolds stress structure.

RESULTS

The Reynolds shear stress structure in the breaker shear layer is shown in Figure 1. Note that positive values in the roller region are not shown to enhance the details in the breaker shear layer. $h_0 = 8.62$cm is the upstream depth, and the origin of the coordinate system is defined at an arbitrary point upstream of the foot of the breaker ($\frac{x}{h_0} = 0.47$). In the following, $\tilde{x} = \frac{x}{h_0}$ and $\tilde{y} = \frac{y}{h_0}$ denote the dimensionless coordinates. The plot shows a coherent shear layer spreading downstream from the foot of the breaker, and has been shown in Misra

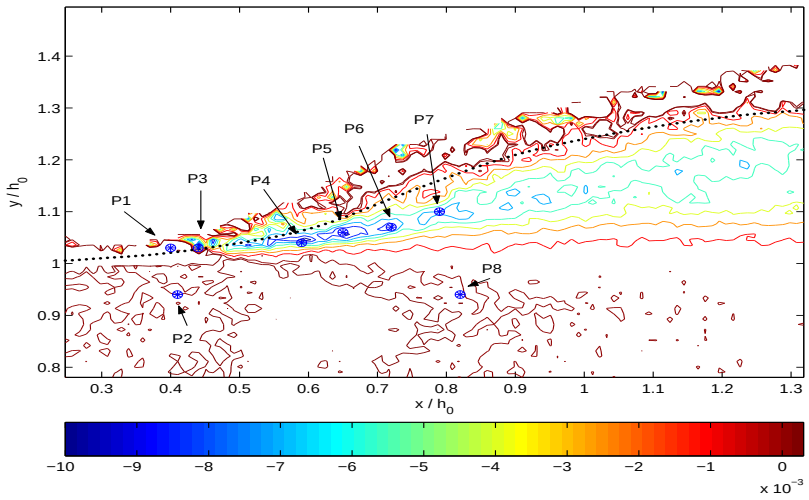

Fig. 1. Contours of ensemble-averaged Reynolds shear stress and location of points chosen for analyzing double correlations

et al. (2005a) to have spreading rates and length scale variations in the streamwise direction in agreement with typical mixing layers. In light of the resolution of the measurement locations ($\Delta\tilde{x} = \Delta\tilde{y} = 0.0102$), we find that there is some marked structure in the (strongly anisotropic) Reynolds shear stress field throughout the shear layer.

Evidence suggests that the eddies that are the most effective in maintaining a correlation between u and v, and in extracting energy from the mean flow through the Reynolds stresses, are vortices whose main axis is roughly aligned with that of the mean strain rate. The correlation coefficient (C_{uv}) defined by Tennekes and Lumley (1972) as

$$C_{uv} \equiv \frac{< uv >}{\sqrt{< u^2 >< v^2 >}} \tag{2}$$

is believed to be $O(1)$ in shear-driven turbulent flows, with $|C_{uv}| \sim 0.4$. The values of C_{uv} obtained in the present case are indeed close to 0.4, with the correlation being consistently higher toward the foot of the breaker (discussed below).

Before we analyze the results of the double spatial correlation, it is instructive to note that the auto-correlation coefficient at zero lag is identically unity, as can be easily verified from equation (1). Also, note that $R_{uv}(x, y, 0, 0) = C_{uv}$, and therefore, at zero lag, the double cross-correlation coefficient should have values around 0.4. Due to computational restrictions, only a truncated section of the whole domain has been analyzed here. Eight distinct locations (shown in Figure 1) of interest in that region are treated as the fixed point and all four correlations (R_{uu}, R_{vv}, R_{uv} and R_{vu}) are calculated for each possible two-dimensional lag within the truncated domain. The locations of the fixed points are: P1(0.4,1.03), P2(0.41,0.94), P3(0.44, 1.03), P4(0.59,1.04), P5(0.65,1.06), P6(0.72,1.07), P7(0.79, 1.10), and P8(0.82,0.94). P1 and P2 are upstream of the foot, with P1 in the intermittent region near the surface. The points P3 - P7 are chosen along the (visually interpreted) centerline of the shear layer in increasing downstream distances from the foot. P8 is below the shear layer and the farthest away from the foot. In Figures 2-9, the horizontal and vertical axes denote the horizontal and vertical lags with respect to the fixed point, with positive and negative horizontal lags signifying downstream and upstream distances respectively. For the

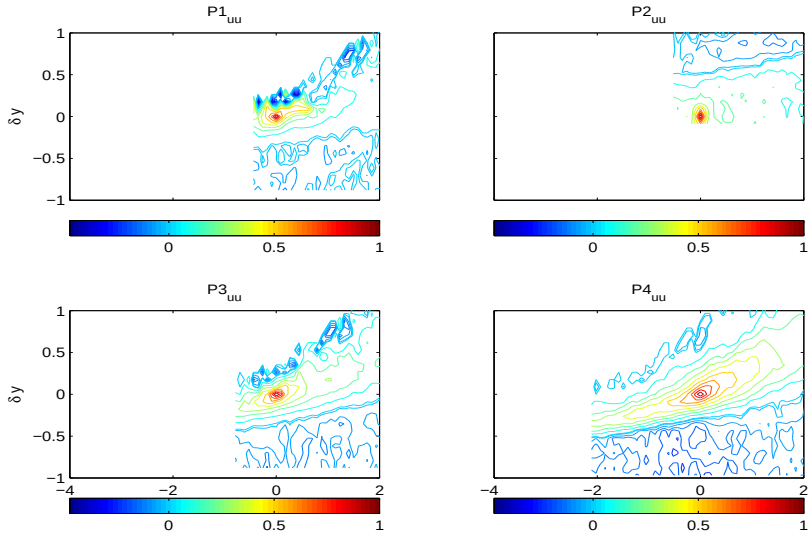

Fig. 2. The double spatial correlation for the horizontal turbulent intensity (u) : R_{uu} at P1, P2, P3 and P4.

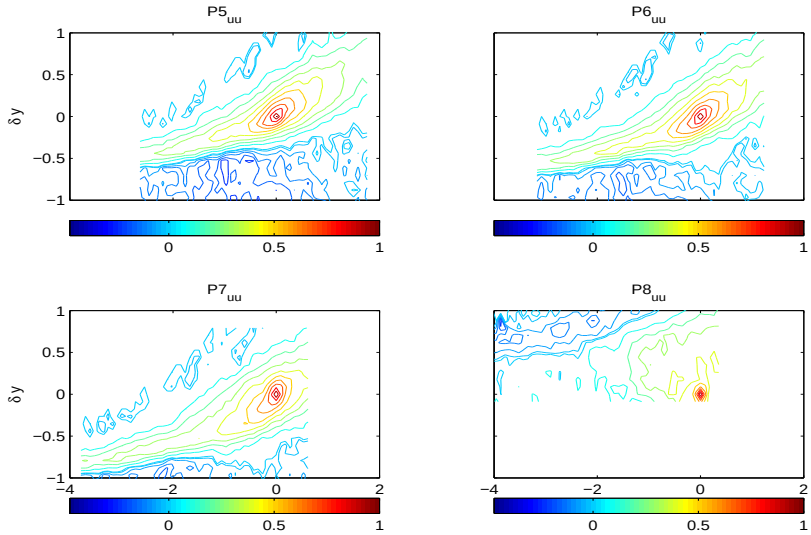

Fig. 3. The double spatial correlation for the horizontal turbulent intensity (u) : R_{uu} at P5, P6, P7 and P8.

vertical lags, positive and negative values signify distances toward the mean surface and bottom respectively. The lags are given in physical units (cm) for easier physical interpretation of the length scales. Positive contour levels are shown at 0.1 increments for each plot except for R_{vu} where they are at 0.04. Negative contour levels are shown at increments of 0.05, except for R_{uu}, where they are at 0.02.

The structure of the turbulence can be determined by analyzing the shape of the correlation coefficients. At P8, below the shear layer, and less than 0.5 h_0 downstream of the foot, the turbulence is (predictably) nearly isotropic, with no preferred orientation for either of the correlation coefficients. The shear layer is thus very localized, even with increasing downstream distance. Similarly, at P2, below the foot of the breaker, there are no indications of

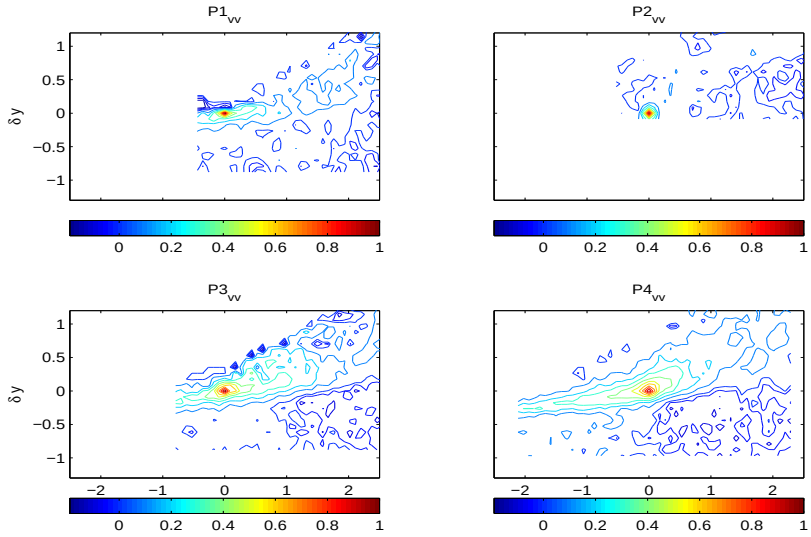

Fig. 4. The double spatial correlation for the vertical turbulent intensity (v) : R_{vv} at P1, P2, P3 and P4.

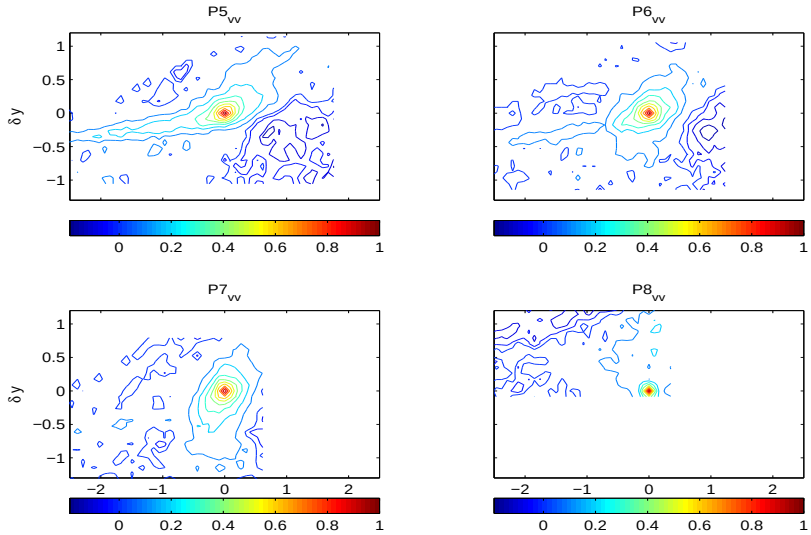

Fig. 5. The double spatial correlation for the vertical turbulent intensity (v) : R_{vv} at P5, P6, P7 and P8.

any large scale coherence. The positive and negative values seen for R_{uu} at P1 are possibly due to the oscillation of the toe, which has been commonly observed in experiments of quasi-steady breakers (Duncan, 1981; Banner, 1988). Note that the values for $R_{uv}(0,0)(=C_{uv})$ are closer to the typical value (0.4) for shear layers in the downstream region, but higher (0.6) close to the foot of the breaker. This is due to the enhanced turbulence generated near the foot from the breaking as well as the presence of an adverse pressure gradient, which distinguish the breaker shear from typical zero-pressure gradient shear layers (Brocchini *et al.*, 2005; Misra *et al.*, 2005a). In this region, however, there are no significantly large negative values, indicating the absence of strictly two-dimensional eddies or vortices in the streamwise-cross-stream plane. P3-P7 show significant packets of coherence throughout the shear layer, with the structures elongated and parallel to the surface near the foot and increasingly compact

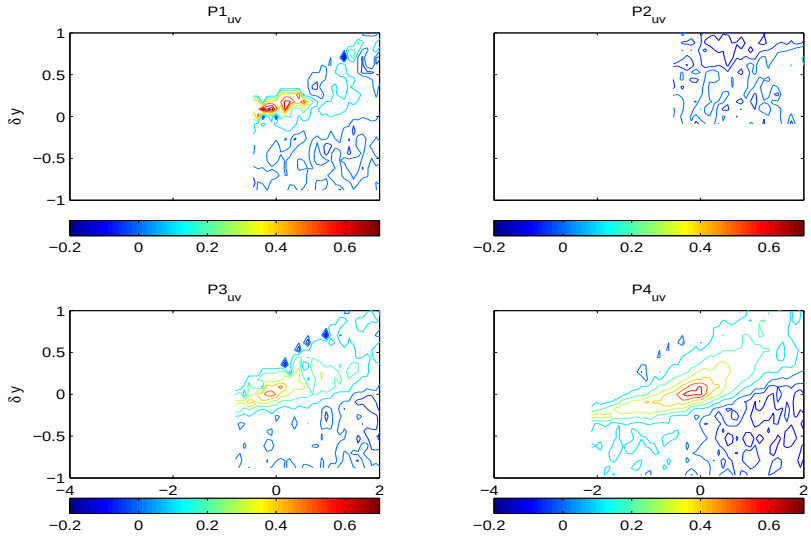

Fig. 6. The cross-correlation R_{uv} at P1, P2, P3 and P4.

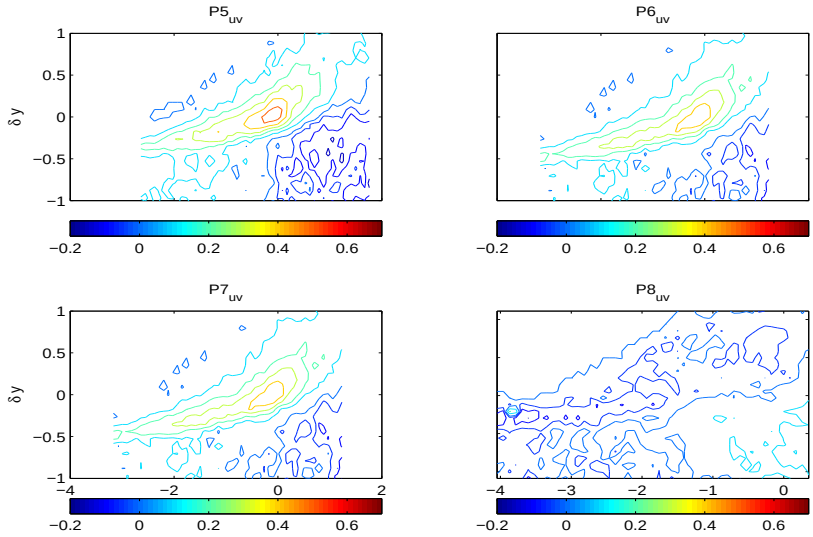

Fig. 7. The cross-correlation R_{uv} at P5, P6, P7 and P8.

(especially for R_{vv}) and oriented normal to the surface further downstream, around $\tilde{x} \sim 0.8$. It is fairly well established that vortex stretching is associated with the energy transfer from the mean flow to the turbulent stresses. It is important to note that the interaction between the mean flow and the turbulent eddies is three-dimensional. Further, this interaction is modified appreciably in the presence of a free surface, which induces topological changes of the coherent eddies resulting in strong turbulence anisotropy near the surface (Hunt, 1987). The shape of the structures near the foot of the breaker are elliptical, with their major axis aligned along the mean strain rate. As we go further downstream they become more compact and circular in form, losing their capacity to extract energy from the mean flow. This is reflected in the decreasing intensity of the Reynolds shear stress in the downstream region. In P5-P7, the coherence is skewed in the streamwise direction parallel to the mean surface, extending further in the upstream direction than in the downstream direction. To quantitatively comment on the length scales, we have to first choose a cut-off value for each correlation

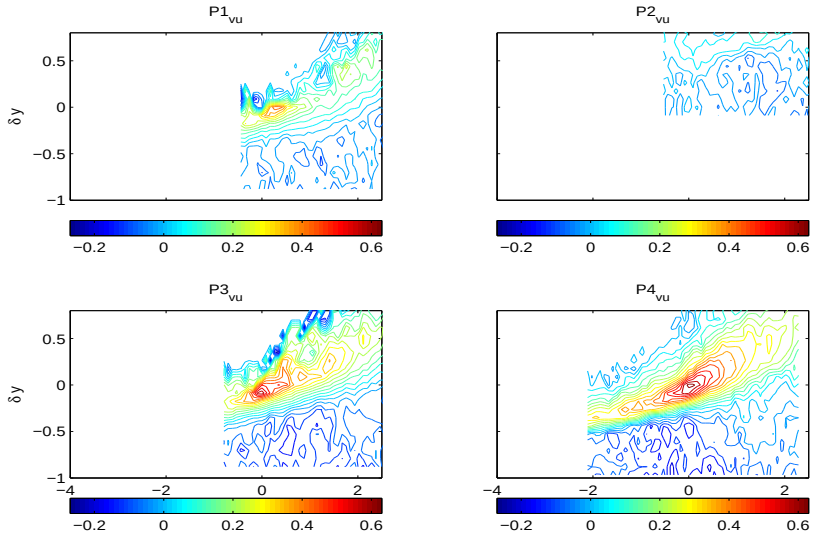

Fig. 8. The cross-correlation R_{vu} at P1, P2, P3 and P4.

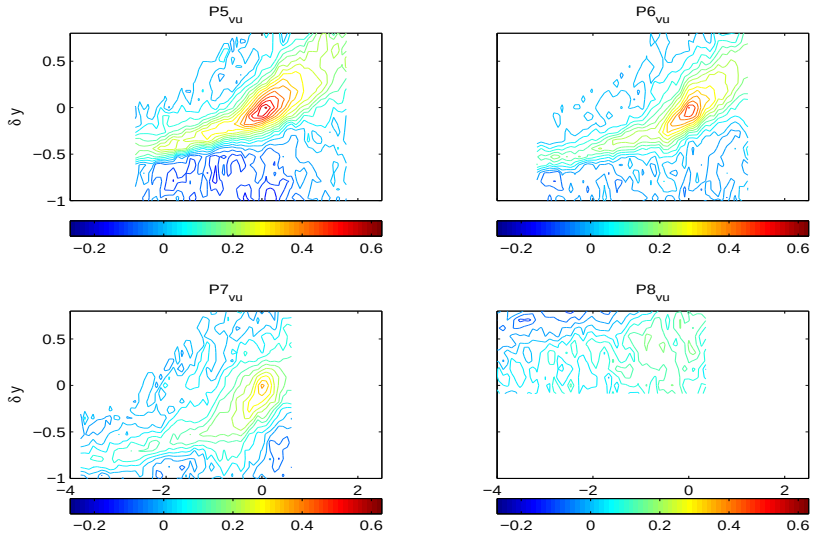

Fig. 9. The cross-correlation R_{vu} at P5, P6, P7 and P8.

coefficient. The contour for this value is therefore used to demarcate the extent of the coherence of the structure. Even though this is highly subjective and depends on the specific flow under investigation, reasonable values can be chosen based on the "background" values found around zero lag at P8, since we know that the turbulence there is nearly isotropic. For R_{uu} and R_{vv}, we, therefore, choose a value of 0.4. For the cross-correlation coefficients, we choose a value of 0.25. The average length scale (l_s in the surface parallel direction) for R_{uu} and both cross-correlations, from P4-P6, is found to be approximately 2.5 cm, with the surface-normal length scale (l_n) being about a quarter of this value. For the vertical correlation, near the foot of the breaker $l_s \sim 2.0$, whereas further downstream, both l_n and l_s are about 0.25 cm. Since the downstream depth $h_1 = 10.85cm$, the height of the breaker is $H_b \equiv h_1 - h_0 = 2.23cm$. Therefore, near the foot of the breaker, $\frac{l_s}{H_b} \sim 1$ whereas further downstream, the ratio for both streamwise and normal length scales, gets smaller with $\frac{l}{H_b} \sim 0.1 - 0.3$. The non-dimensional length scales are, therefore, in the range of values

reported by Longo (2003) and Cox and Anderson (2001). Instead of the breaker height, the upstream water depth can also be chosen as a relevant scale for non-dimensionalizing the turbulent scales, and near the foot of the breaker, $\frac{l_s}{h_0} \sim 0.26$. This is in agreement with Stansby and Feng (2005), who found that the length scales of structures near the surface varied from greater than, to a fraction of the water depth.

CONCLUSIONS

Planar PIV data of a turbulent laboratory hydraulic jump are analyzed with two-point spatial correlations. Eight distinct locations are chosen to look at the different flow regimes. Particular attention is focussed on the coherent structures in the breaker shear layer. The values for the cross-correlation coefficient C_{uv} at the downstream locations are in agreement with typical shear layer values (~ 0.4), whereas they are higher (~ 0.6) closer to the foot of the breaker. The coherence in the shear layer is found to be localized, with the turbulence structure, 3 cm downstream of the toe and 2 cm below the mean free surface, being nearly isotropic. No evidence is found of strictly two-dimensional eddies in the streamwise-cross-stream plane. Instead, elongated packets are found oriented parallel to the mean surface, with the horizontal correlation extent in the upstream direction, decreasing away from the foot of the breaker. It is seen that near the foot of the breaker, and in the streamwise-cross-stream plane, the structures are ellipses, with their major axes oriented along the mean shear and therefore, most efficient in extracting energy from the mean flow. Further downstream, the structures are more compact and circular. Near the foot of the breaker, the length scales are approximately equal to the height of the breaker, whereas, further downstream, the ratio $\frac{l}{H_b} \sim 0.1 - 0.3$, in reasonable agreement with the range of values reported by Cox and Anderson (2001) and Longo (2003).

ACKNOWLEDGEMENTS

S. K. Misra and J. T. Kirby acknowledge the support of the National Oceanographic Partnership Program (NOPP).

REFERENCES

Banner, M. L. (1988). Surging characteristics of spilling zones of quasi-steady breaking water waves. In K. Horikawa and H. Maruo, editors, *Nonlinear Water Waves*, IUTAM Symposium, pages 151–158. Natl. Academic.

Battjes, J. A. and Sakai, T. (1981). Velocity field in a steady breaker. *J. Fluid Mech.*, **111**, 421–437.

Brocchini, M. and Peregrine, D. H. (2001). The dynamics of turbulent free surfaces. part 1. Description. *J. Fluid Mech.*, **449**, 225–254.

Brocchini, M., Misra, S. K., Peregrine, D. H., and Kirby, J. T. (2005). The dynamics of turbulent free surfaces. Part 3. A model for spilling breaking waves. In Preparation.

Chang, K. and Liu, P. L. (1998). Velocity, acceleration and vorticity under a breaking wave. *Phys. Fluids*, **10**(1), 327–329.

Cointe, R. and Tulin, M. P. (1994). A theory of steady breakers. *J. Fluid Mech.*, **276**, 1–20.

Cox, D. T. and Anderson, S. L. (2001). Statistics of intermittent surf zone turbulence and observations of large eddies using piv. *Coast. Engrng. J.*, **43**(2), 121–131.

Duncan, J. H. (1981). An experimental investigation of breaking waves roduced by a towed hydrofoil. *Proc. R. Soc. Lond. Series A*, **377**, 331–348.

Duncan, J. H. (2001). Spilling breakers. *Ann. Rev. Fluid Mech.*, **33**, 519–547.

Ganapathisubramani, B., Hutchins, N., Hambleton, W. T., Longmire, E. K., and Marusic, I. (2005). Investigation of large-scale coherence in a turbulent boundary layer using two-point correlations. *J. Fluid Mech.*, **524**, 57–80.

Govender, K., Mocke, G., and Alport, M. (2002). Video imaged surf zone wave and roller structures and flow fields. *J. Geophys. Res.*, **107**(C10), 3177.

Hunt, J. C. R. (1987). Turbulent structure and turbulent diffusion near gas-liquid interfaces. In W. Brutsaert and G. H. Girka, editors, *Gas transfer at water surfaces*, pages 67–82. Reidel, Dordrecht.

Longo, S. (2003). Turbulence under spilling breakers using discrete wavelets. *Exp. Fluids*, **34**, 181–191.

Madsen, P. A. and Svendsen, I. A. (1983). Turbulent bores and hydraulic jumps. *J. Fluid Mech.*, **129**, 1–25.

Melville, W. K., Veron, F., and White, C. J. (2002). The velocity field under breaking waves: coherent structures and turbulence. *J. Fluid Mech.*, **454**, 203–233.

Misra, S. K., Kirby, J. T., Brocchini, M., Veron, F., Thomas, M., and Kambhamettu, C. (2005a). Hydraulic jump as a quasi-steady spilling breaker - an experimental analysis of similitude. *J. Fluid Mech.*. Under peer review.

Misra, S. K., Thomas, M., Kambhamettu, C., Kirby, J. T., Veron, F., and Brocchini, M. (2005b). Estimation of complex air-water interfaces from piv images. *Exp. Fluids*. Under peer review.

Nadaoka, K. (1986). A fundamental study on shoaling and velocity field structure of water waves in the nearshore zone. Technical Report 36, Dept. of Civil Engrng, Tokyo Inst. of Tech.

Peregrine, D. H. and Svendsen, I. A. (1978). Spilling breakers, bores and hydraulic jumps. In *Proceedings of the 16th ICCE, Hamburg*, pages 540–555. ASCE.

Stanislas, M., Carlier, J., Foucaut, J.-M., and Dupont, P. (1999). Double spatial correlation, a new experimental insight into wall turbulence. *C. R. Acad. Sci. Paris*, **327**(II b), 55–61.

Stansby, P. and Feng, T. (2005). Kinematics and depth-integrated terms in the surf zone waves from laboratory measurement. *J. Fluid Mech.*, **529**, 279–310.

Svendsen, I. A. and Madsen, P. A. (1984). A turbulent bore on a beach. *J. Fluid Mech.*, **148**, 73–96.

Tennekes, H. and Lumley, J. L. (1972). *A first course in turbulence*. MIT Press.